Complex Formation in Solutions of Oppositely Charged Polyelectrolytes at Different Polyion Compositions and Salt Content†

Yoshikatsu Hayashi,* Magnus Ullner, and Per Linse

Physical Chemistry 1, Center for Chemistry and Chemical Engineering, Lund University, P.O. Box 124, S-221 00 Lund, Sweden

Received: November 26, 2002; In Final Form: May 7, 2003

The formation of complexes in solutions containing positively charged polyions (polycations) and a variable amount of negatively charged polyions (polyanions) has been investigated by Monte Carlo simulations. The polyions were described as flexible chains of charged hard spheres interacting through a screened Coulomb potential. The systems were analyzed in terms of cluster compositions, structure factors, and radial distribution functions. At 50% charge equivalence or less, complexes involving two polycations and one polyanion were frequent, while closer to charge equivalence, larger clusters were formed. Small and neutral complexes dominated the solution at charge equivalence in a monodisperse system, while larger clusters again dominated the solution when the polyions were made polydisperse. The cluster composition and solution structure were also examined as functions of added salt by varying the electrostatic screening length. The observed formation of clusters could be rationalized by a few simple rules.

1. Introduction

Solutions containing both positively and negatively charged polyions (in the following referred to as polycations and polyanions, respectively) have gained much interest recently. The strong Coulomb interaction between the oppositely charged polyions leads to a strong association. This association often initiates an associative phase separation, resulting in one polymer-rich and one polymer-poor phase.

Kabanov and co-workers[1−5] carried out comprehensive studies of soluble polyion complexes including the preparation conditions of the complexes, their structure and kinetics, as well as exchange reactions between polyion complexes and other polyions as a function of polyion properties and salt concentration. Pogodina and Tsvetkov[6] studied the formation of complexes in solutions of oppositely charged polyelectrolytes over a wide range of mixing ratios. At a specific mixing ratio, they observed a simultaneous increase in mass, size, and polymer density of the polyion complexes formed. The interaction between DNA and oppositely charged polyions is of great interest in molecular biology. Single DNA molecules can be studied by fluorescence microscopy. Yoshikawa and co-workers, for example, observed the compaction of DNA in the presence of short, flexible cations, such as spermidine (trivalent) and spermine (tetravalent),[7−9] as well as with polycations, namely, polyalginate.[10,11] They discussed the mechanism of compaction in terms of a first-order phase transition. Finally, the formation of alternating layers of polycations and polyanions at solid surfaces,[12,13] originally developed by Decher and co-workers, is another and rapidly expanding area that involves mixtures of polyions.[14]

To elucidate the general tendencies of the influence of salt on polyelectrolyte complex formation, Dautzenberg[15] studied this process by static light scattering as a function of the ionic strength of the medium and the molar ratio of the solution components. He reported that in most systems the internal structure of the complexes is marginally affected by salt. However, he also concluded that a prediction of the effects of salt during complex formation is very difficult, because the process depends on the specific characteristics of the polyelectrolyte components.

In simulation studies, flexible polyions are normally modeled as linear chains of charged beads in a dielectric continuum. Simple ions are either included explicitly or implicitly using a screened Coulomb potential as an effective interaction between chain beads. Christos and Carnie[16] simulated polyelectrolyte solutions in the presence of added salt using the screened Coulomb potential. Later, Stevens and Kremer presented a series of investigations of salt-free polyelectrolyte solutions with explicit ions[17−19] and made comparisons with a screened Coulomb model.[20] Such comparisons have also been made based on simulations of single chains.[21−24] As for systems of oppositely charged polyelectrolytes, Winkler et al.[25] investigated the structure of two flexible, oppositely charged polyions as a function of the interaction strength between the chain beads. They found scaling exponents for the radius of gyration and also reported that, as soon as the interaction is strong enough, the systems collapse to form very compact structures with a distinct spherical surface and pronounced local order.

Our aim is to improve our understanding of the complex formation in solutions of oppositely charged polyions using Monte Carlo simulations. In a previous paper,[26] we investigated the properties of solutions of polycations with different amounts of polyanions up to 50% charge equivalence. Two different linear charge densities were considered, and structure factors, radial distribution functions, and polyion extensions were determined. Two models were used: one involving only polyions with the beads interacting via a screened Coulomb potential and another where explicit small ions were included and all charges interacted through a Coulomb potential. We concluded that the results were qualitatively the same for the

† Part of the special issue "International Symposium on Polyelectrolytes".

10.1021/jp022491a CCC: $25.00
Published on Web 07/11/2003

two models, and for polyion conformations within a complex, the agreement was even quantitative.

In this contribution, we extend our study to compositions of the two polyions up to charge equivalence. Near charge equivalence, the investigated systems form extensive polyion complexes. In particular, cluster composition and the structure of the solutions are investigated. Moreover, the effect of added salt is examined.

The outline of this paper is as follows: section 2 describes the model, and some simulation aspects are given in section 3. An introduction to structure factors is given in section 4. Our results are given in section 5, where we report on the formation of polyion complexes as a function of the polyion composition and screening length, observed through cluster composition analysis, structure factors, and radial distribution functions. The paper ends with conclusions given in section 6.

2. Model

We used a simple model that represents polyelectrolyte solutions containing charged polyions and small ions in an aqueous medium. The polyions are described as freely jointed chains with charged hard spheres (beads) connected by harmonic bonds. The electrostatic interactions are described by a screened Coulomb potential, which treats the small ions and the solvent implicitly. In our previous study, we found that a screened Coulomb potential provides a reasonable description of the effects of the small ions.

The total interaction energy U of the system is given by

$$U = \sum_{i<j}^{n_{pos}+n_{neg}} u_{nonbond,ij} + \sum_{m=1}^{N_{pos}+N_{neg}} \sum_{i=1}^{N_{bead,m}-1} u_{bond,m,i} \qquad (1)$$

where the separate contributions are pairwise additive and n_{pos} and n_{neg} represent the total number of positive and negative beads, respectively. N_{pos} and N_{neg} denote the number of polycations and polyanions, respectively, and $N_{bead,m}$ is the number of beads in chain m. The interaction potential $u_{nonbond,ij}$ for a pair ij, where i and j are any two beads, is given by

$$u_{nonbond,ij}(r_{ij}) = \begin{cases} \infty & r_{ij} < R_i + R_j \\ z_i z_j k_B T l_B \dfrac{\exp(-\kappa r_{ij})}{r_{ij}} & r_{ij} \geq R_i + R_j \end{cases} \qquad (2)$$

where z_i is the valence of bead i, k_B is Boltzmann's constant, T is the temperature, R_i is the radius of bead i, and r_{ij} is the distance between the centers of beads i and j. The Bjerrum length is defined as

$$l_B = \frac{e^2}{4\pi\epsilon_0\epsilon_r k_B T} \qquad (3)$$

where e is the elementary charge, ϵ_0 the permittivity of vacuum, and ϵ_r the relative permittivity of the solvent. Moreover, κ denotes the inverse Debye screening length given by

$$\kappa^2 = 4\pi l_B \sum_k z_k^2 \rho_k \qquad (4)$$

where the summation extends over the implicit small ions (counterions and added salt species) with ρ_k denoting the number density of small ions of type k. The bond potential $u_{bond,m,i}$ is given by the harmonic potential

TABLE 1: Overview of the Salt-Free Systems with Screening Lengths and Root-Mean-Square Displacements of Polycations and Polyanions

label	N_{neg}	κ^{-1}/Å	$\langle \Delta \mathbf{r}_{pos}^2 \rangle^{1/2}/L_{box}$	$\langle \Delta \mathbf{r}_{neg}^2 \rangle^{1/2}/L_{box}$
system 0	0	14.8	31.7	
system 5	5	12.1	9.7	5.2
system 9	9	10.7	3.6	4.4
system 10	10	10.5	5.1	4.2

TABLE 2: Number of Chains with Different Number of Beads N_{bead} Representing the Polydisperse Systems (the same distribution was used for polycations and polyanions)

	N_{bead}				
label	16	18	20	22	24
system 181		1	8	1	
system 262		2	6	2	
system 12421	1	2	4	2	1

$$u_{bond,m,i} = \frac{k_{bond}}{2}(r_{m;i,i+1} - r_0)^2 \qquad (5)$$

where $r_{m;i,i+1}$ is the distance between beads i and $i+1$ belonging to polyion m. An equilibrium bond length $r_0 = 5$ Å is used with a force constant $k_{bond} = 0.4$ N/m. With the other interactions included, the root-mean-square (rms) bead-to-bead separation is typically 5.9 Å.

Throughout, monovalent beads, i.e., $z_i = \pm 1$, with a common radius $R_i = 2$ Å are used. Unless otherwise stated, polyions have $N_{bead} = 20$ beads. Systems containing $N_{pos} = 10$ polycations and $N_{neg} = 0$, 5, 9, or 10 polyanions are considered, and they will be referred to as system 0, system 5, system 9, and system 10, respectively. A few systems related to system 10 involving (i) length (and hence charge) polydispersity and (ii) polycations and polyanions of unequal length (and hence of unequal absolute charge) are also considered. In eq 4, ρ_k for the salt-free systems is calculated from the number of monovalent counterions to the polyions; i.e., the implicit number of small ions is the sum of $N_{bead}N_{neg}$ cations and $N_{bead}N_{pos}$ anions. The effect of adding salt is modeled by giving the Debye screening length κ^{-1} a lower value than in the salt free-systems.

The simulations were performed at $T = 298$ K using $\epsilon_r = 78.5$, representing water as the solvent ($l_B = 7.14$ Å). Tables 1 and 2 provide an overview of investigated systems as well as the Debye screening length κ^{-1} of the salt-free systems.

3. Simulation Method

The equilibrium properties of the model systems were obtained by employing canonical Monte Carlo simulations according to the Metropolis algorithm,[27,28] using the integrated Monte Carlo/molecular dynamics/Brownian dynamics simulation package MOLSIM.[29] The polyions were enclosed in a cubic box with a box length $L_{box} = 158$ Å, and periodic boundary conditions were applied. A spherical cutoff at $L_{box}/2$ was employed for the screened Coulomb interactions.

Due to the strong complexation between oppositely charged polyions, the selection of trial moves is important for adequate sampling. The polyions were subjected to four types of trial displacements, viz. (i) translation of a single bead, (ii) slithering move, (iii) pivot rotation, and (iv) translation of an entire chain. The selection among the four different trial moves was made randomly using the weights 0.4, 0.3, 0.1, and 0.2, respectively.

The chains were initially placed randomly in the simulation box. The equilibration involved 3×10^5 passes (trial moves per bead), and the production runs were 9×10^5 passes. The rms displacements of individual beads during the production

runs are given in Table 1. Despite the strong electrostatic interactions in the complexes formed, the smallest rms displacement is 4 times the box length, indicating an adequate sampling. Statistical uncertainties are given as one standard deviation of the mean and were estimated by dividing the simulation into 10 subbatches.

Further details on the protocol and convergence of simulations of these systems are available in ref 26.

4. Structure Factors

Structure factors have been calculated to characterize the structure of the systems. Throughout, only partial structure factors concerning polycations will be given.

The partial structure factor $S_{pos}(q)$ involving the positively charged beads is defined as

$$S_{pos}(q) = \left\langle \frac{1}{n_{pos}} \left| \sum_{j=1}^{n_{pos}} \exp(i\mathbf{q}\cdot\mathbf{r}_j) \right|^2 \right\rangle \quad (6)$$

where $\mathbf{q}$ is a wave vector with magnitude q, $\mathbf{r}_j$ is the position of positive bead j, n_{pos} is the total number of positive beads, and $\langle ... \rangle$ denotes an ensemble average. In particular, the change of the structure as polyanions are added to the solution of polycations will be of interest. The structure factor $S(q)$ is proportional to the scattering intensity $I(q)$, which can be observed experimentally. In, e.g., neutron scattering, it is possible to observe a partial structure factor by selective isotope substitution.

If intra- and interpolyion correlations can be considered as statistically independent, the structure factor becomes a product of a polycation form factor, $F_{pos}(q)$, and a polycation structure factor with respect to the centers of mass, $S_{pos,CM}(q)$, according to

$$S_{pos}(q) = F_{pos}(q) S_{pos,CM}(q) \quad (7)$$

The form factor, describing the average shape of the chains, depends only on intrapolycation correlations and is given by

$$F_{pos}(q) = \frac{1}{N_{pos}} \sum_{m=1}^{N_{pos}} \left\langle \frac{1}{N_{bead,m}} \left| \sum_{j=1}^{N_{bead,m}} \exp(i\mathbf{q}\cdot\mathbf{r}_{m,j}) \right|^2 \right\rangle \quad (8)$$

where $N_{bead,m}$ denotes the number of beads in polycation m and N_{pos} is the number of polycations. The polycation structure factor, $S_{pos,CM}(q)$, depends only on interpolycation correlations and is given by

$$S_{pos,CM}(q) = \left\langle \frac{1}{N_{pos}} \left| \sum_{m=1}^{N_{pos}} \exp(i\mathbf{q}\cdot\mathbf{r}_{CM,m}) \right|^2 \right\rangle \quad (9)$$

where $\mathbf{r}_{CM,m}$ denotes the center-of-mass coordinate of polycation m. Comparison of $S_{pos}(q)$ calculated from eq 6 or eqs 7−9 indicates whether there is any correlation between the polycation conformation and the cluster formation.

The partial structure factor, $S_{pos}(q)$, is related to the thermodynamic characteristics of the system when it is viewed as a solution of independent (disconnected) positive beads. In the same way, the center-of-mass structure factor, $S_{pos,CM}(q)$, reflects the properties of a system where polycations are the only observable solutes. In the limit $q \to 0$, $S_{pos,CM}(q)$ approaches the partial osmotic compressibility, $\kappa_{T,pos}$, of the solution of polycations according to

$$\lim_{q\to 0} S_{pos,CM}(q) = k_B T \left(\frac{\partial \Pi_{pos}}{\partial c_{pos}} \right)^{-1}_{N_{pos},T} = \rho_{pos} k_B T \kappa_{T,pos} \quad (10)$$

where Π_{pos} is the osmotic pressure contribution from polycations and ρ_{pos} the number density of polycations. A divergence of $\lim_{q\to 0} S_{pos,CM}(q)$ is equivalent to a divergence of $\kappa_{T,pos}$, signaling a phase separation.

In our simulations, the value of q for the structure factors has a lower limit determined by the finite box size according to $q_{low} = 2\pi/L_{box}$. Thus, $\lim_{q\to 0} S_{pos,CM}(q)$ cannot be obtained, but a net interaction between polycations can still be discussed in terms of the behavior of the partial structure factor at $q = q_{low}$. A steadily increasing $S_{pos,CM}(q)$ as $q \to q_{low}$ does not necessarily mean that the system wants to phase separate, but it does show that there are attractive interactions and aggregation. Repulsive interactions, on the other hand, cause $S_{pos,CM}(q)$ to decrease when $q \to q_{low}$.

5. Results and Discussion

5.1. No Added Salt. *5.1.1. Overview.* It is expected that the structure of the polyelectrolyte solution depends on the number of oppositely charged polyelectrolytes added. The final configurations of simulations with $N_{pos} = 10$ polycations and $N_{neg} = 0$, 5, 9, and 10 polyanions are displayed in Figure 1. With only polycations, a homogeneous polyelectrolyte solution is observed (Figure 1a). The polyions are stretched by electrostatic *intra*chain repulsion and are well separated by electrostatic *inter*chain repulsion. As polyanions are added, complexes containing at least one polycation and one polyanion are formed. In the case of $N_{neg} = 5$, all polycations (as well as all polyanions) appear to be complexed (Figure 1b). Five separate complexes are discernible, each complex containing two polycations and one polyanion. With $N_{neg} = 9$, the snapshot shows two complexes, one containing nine polycations and eight polyanions and another made up of the remaining two polyions of opposite charge (Figure 1c). Finally, with $N_{neg} = 10$, several (neutral) complexes are found (Figure 1d). Thus, the polyelectrolyte solution appears to undergo large structural changes as oppositely charged polyions are added and near or at charge equivalence complexes of different compositions appears.

5.1.2. Cluster Composition. The compositions of complexes formed have been examined by calculating distribution functions that show the probabilities of all possible combinations of polyions. Two polyions are considered to belong to the same cluster if they are "connected" directly or indirectly through one or several other polyions. Two polyions are directly connected if their center-of-mass separation does not exceed 30 Å. A cluster is classified according to how many polycations and polyanions it contains. From the simulations, the cluster size probability distribution $P_{m,n}$ was calculated according to

$$P_{m,n} = \frac{(m+n)\langle n_{m,n}{}^{cluster} \rangle}{\sum_m \sum_n (m+n)\langle n_{m,n}{}^{cluster} \rangle} \quad (11)$$

where $\langle n_{m,n}{}^{cluster} \rangle$ is the average number of clusters containing m polycations and n polyanions. Note that $P_{m,n}$ is a "mass"-weighted measure of the cluster size distribution, where the number of chains $(m + n)$ in a cluster provides the weight. It represents the probability that any polyion, chosen randomly among both polycations and polyanions, will be found in a cluster of type m:n. In other words, it shows how the polyions are distributed between different clusters.

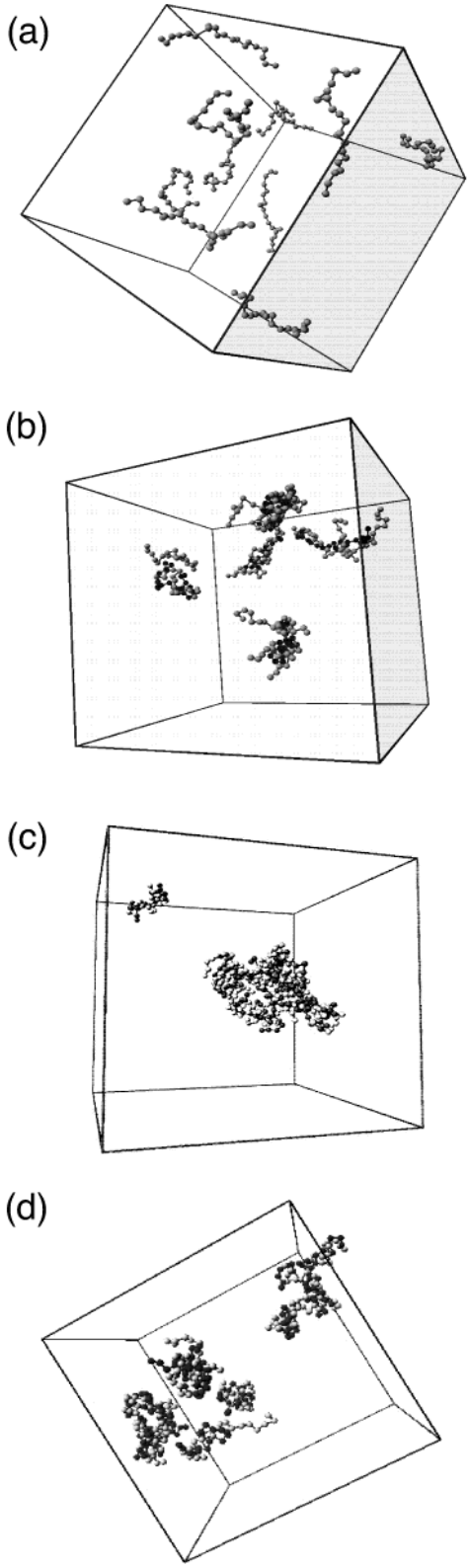

Figure 1. Final configurations of (a) system 0, (b) system 5, (c) system 9, and (d) system 10. The systems contain 10 polycations composed of 20 positively charged beads (gray spheres) and 0, 5, 9, and 10 polyanions, respectively, composed of 20 negatively charged beads (black spheres). Some beads have been translated in accord with the periodic boundary conditions (one box length) to better illustrate the cluster formation. The simulation boxes have been rotated to give the clearest view in each case.

Figure 2 shows the distribution of $P_{m,n}$ as a function of m and n for system 5, system 9, and system 10. Briefly, in system 5 the 2:1 cluster is the dominating one (Figure 2a), in system 9

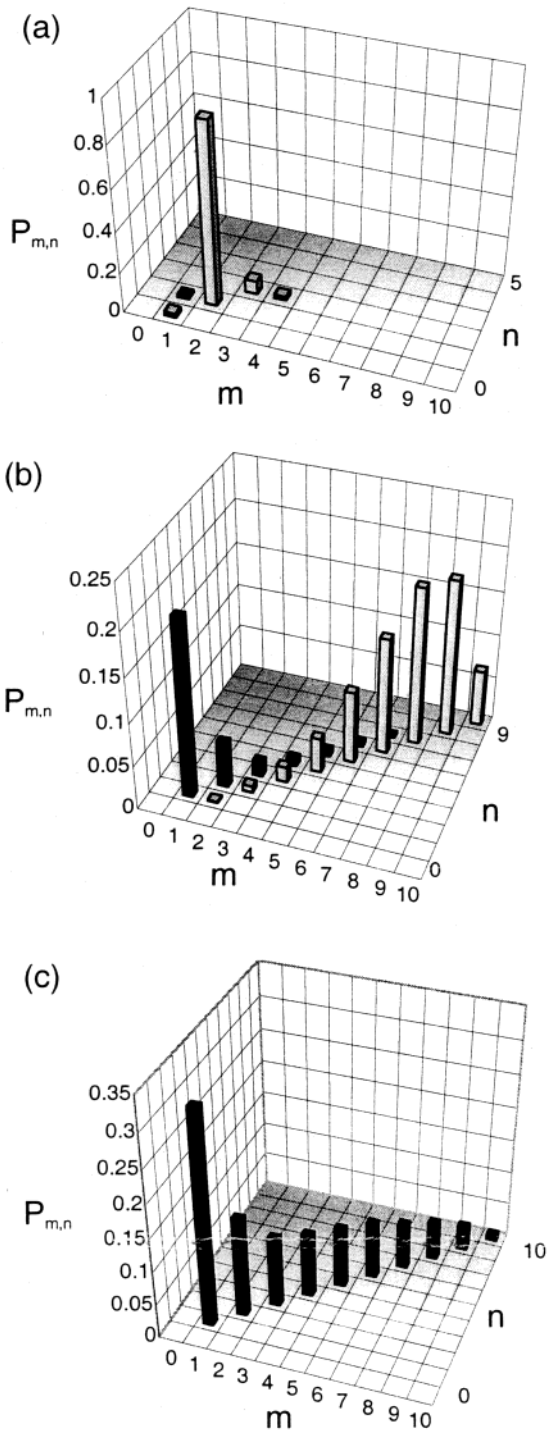

Figure 2. Cluster size probability distribution $P_{m,n}$ vs the number of polycations m and the number of polyanions n in polyion complexes for (a) system 5, (b) system 9, and (c) system 10. Neutral clusters are represented by black columns and charged clusters by gray columns.

large charged clusters coexist with small neutral clusters (Figure 2b), whereas in system 10 neutral clusters are found with a preference for smaller ones (Figure 2c). In the two latter systems, considerable fluctuations in the cluster sizes occur.

The distribution of clusters can be rationalized by four simple rules. They are as follows: (I) coexistence of oppositely charged clusters is avoided to gain favorable electrostatic potential energy, (II) the cluster net charge density (cluster net charge divided by cluster size) is minimized to reduce the electrostatic repulsion among excess charges, (III) the total net charge (the number of excess polyions in a cluster) is kept low for the same

reason, and (IV) the number of clusters is maximized to gain translational entropy. In this context, an uncomplexed (referred to as free) polyion is also treated as a cluster. Rules I−III could be combined into one, but the purpose is to illustrate trends rather than to give a compact description.

Rule II promotes larger clusters, while rule IV favors a larger number of smaller clusters. Rule III also works against the formation of large (highly charged) clusters, but the main energy−entropy balance of the system can be represented by rules II and IV in a simplified discussion, assuming that rule I is satisfied. Under the constraint of the stoichiometric ratio of polycations and polyanions, each system will minimize its free energy by establishing the most favorable complex composition for the conditions given by κ^{-1}, box volume, temperature, etc.

The cluster size probability distributions will now be examined in more detail and how they comply with these rules, in particular, the balance between the antagonistic rules II and IV. We will start with a pure polyelectrolyte solution (system 0) and end with charge equivalence of the two oppositely charged polyions (system 10).

In system 0, we have only free polycations, $P_{1,0} \approx 1$. As polyanions are added, the fraction of free polycations is reduced and the fraction of 2:1 clusters is increased. The cluster size probability distribution for system 5 displays an overwhelming dominance of the 2:1 cluster (Figure 2a). Comparing the formation of a 2:1 cluster with the alternative of separate 1:0 and 1:1 clusters, rule II states that it is more favorable to share the excess charge of one polycation among the three polyions in a 2:1 cluster than to have the excess charge localized in a free polycation, while rule IV would favor separation. Apparently, rule II takes precedence over rule IV.

For system 5, another alternative would be one 10:5 cluster comprising all polyions instead of five 2:1 clusters. The screening length is fairly short compared to a complex, and we will use a simple mean-field approximation to analyze the situation. If electrostatic pair interactions are represented by the volume l_B/κ^2 (ignoring numerical constants), which is just an integral over the (dimensionless) screened Coulomb potential, the electrostatic energy of a m:n cluster is

$$\beta U_{m,n} \sim \frac{l_B Z^2}{\kappa^2 V} \sim \frac{l_B (m-n)^2}{\kappa^2 (m+n)} \tag{12}$$

where $\beta \equiv 1/k_B T$. In the last step we used a net charge $Z = m - n$ in terms of polyions and assumed that the volume V is proportional to the total number of polyions in the cluster. If we make a multiple λm:λn of m:n clusters, where λ is an integer, we see that the energy per member $\beta U_{m,n}/\lambda$ is independent of λ. In other words, sharing the charges of 5 excess polycations among 15 polyions is not much different from sharing charges of 1 excess polycation among 3 polyions in a 2:1 cluster. By this argument, a rearrangement is neutral with respect to rule II, while rule IV dictates that five 2:1 clusters is better than one 10:5 cluster and the latter should be suppressed. This is also what we observe in the simulations.

With eq 12 representing rule II, much of the results can be explained as a balance between rules II and IV, but it is not the whole truth. There is also an energetic component that favors clusters with a smaller net charge among clusters with the same ratio of polycations and polyanions. This is rule III and to rationalize it, we may consider the unscreened limit. If a cluster is seen as a charged sphere of radius R, we have

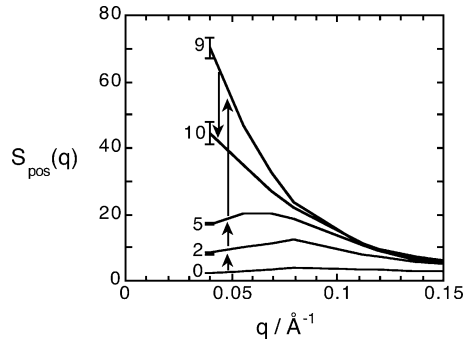

Figure 3. Partial structure factors of positive beads $S_{pos}(q)$ for the indicated systems. Statistical uncertainties, which decrease as q is increased, are given at $q = q_{min}$. The arrows show the order of increasing amounts of polyanions.

$$\beta U_{m,n} \approx \frac{l_B Z^2}{R} \approx \frac{l_B (m-n)^2}{(m+n)^{1/3}} \tag{13}$$

with the specific energy $\beta U_{m,n}/\lambda$ of a λm:λn cluster growing as $\lambda^{2/3}$. Hence, highly charged clusters are disfavored. The true behavior should lie somewhere between the limits represented by eqs 12 and 13. We will return to eqs 12−13 and to rule III in the context of added salt.

In system 9, clusters of different compositions appear, mainly large charged clusters coexisting with small neutral ones (Figure 2b). According to rule II, it is most favorable to distribute the excess polycation charge in a large cluster by adding as many neutral polycation-polyanion pairs as possible. This is the dominating principle, although rule IV receives a concession through the preference of a system with one 9:8 and one 1:1 cluster over the formation of one cluster with the maximum cluster size 10:9 (see also Figure 1c).

Finally, in system 10 with charge equivalence of the two oppositely charged polyions, only neutral and preferentially small to intermediate sized clusters appear with the largest probability for the 1:1 cluster. Here, the appearance of any kind of charged cluster would require the formation of an oppositely charged cluster, which would violate rule I. Since only neutral clusters occur, such charge separation is indeed very unfavorable. According to rule IV, we would expect a dominance of 1:1 clusters, which is borne out by Figure 2c. Although the largest probability is obtained for a 1:1 cluster, larger clusters appear also (see also Figure 1d). These larger clusters are promoted by an increasingly negative (favorable) cohesive electrostatic energy occurring in larger electroneutral clusters, which will be demonstrated below.

5.1.3. Solution Structure. Figure 3 displays the partial structure factors for positively charged beads. At $q = q_{low}$, the general trend is that $S_{pos}(q)$ grows as the number of polyanions is increased. The growth of the structure factor at small q indicates increasing long-ranged spatial correlations among positive beads and quantifies the spatial inhomogeneity displayed in the snapshots (Figure 1). However, system 10 constitutes an exception, the structure factor at small q being smaller than that for system 9. Obviously, the spatial inhomogeneity is largest for system 9, also being consistent with the snapshots given in Figure 1.

The partial structure factors for systems 0−5 display a maximum at $q \approx 0.07-0.09$ Å^{-1}, indicating that collections of positively charged beads remain well separated. The growth of the maximum as N_{neg} is increased reflects the increasing number of positively charged beads located in clusters containing more than one polycation. Moreover, the shift of the maximum to

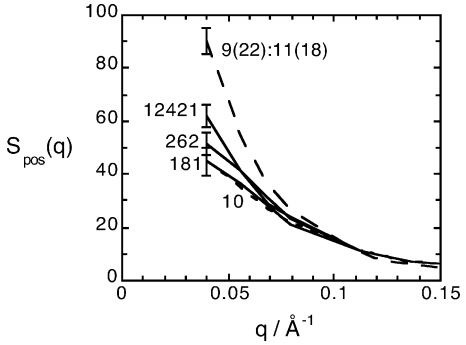

Figure 4. Partial structure factors of positive beads $S_{pos}(q)$ for system 10 (short-dashed line), the indicated polydisperse systems (solid lines), and the system with polycations and polyanions of unequal length and hence of unequal absolute charges (long-dashed line). Statistical uncertainties, which decrease as q is increased, are given at $q = q_{min}$.

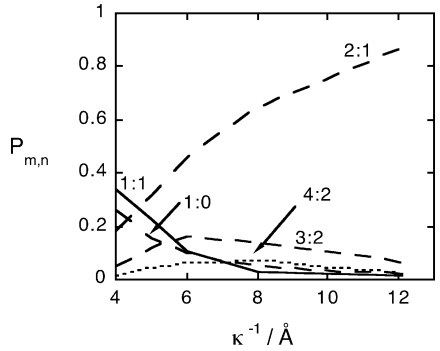

Figure 5. Cluster size probability distribution $P_{m,n}$ vs screening length κ^{-1} for system 5 and selected cluster compositions as indicated. The neutral 1:1 cluster is given as a solid line, and charged clusters are represented by dashed (one excess polycation) and dotted (two excess polycations) lines.

smaller q as N_{neg} is increased shows that the average separation between the collections of positive beads is increased, consistent with a depletion of free polyions in favor of complexes, leading to fewer collections with a larger mean separation.

In system 9 there is more than one neutral polycation−polyion pair for each excess polycation. These pairs are collected into larger clusters by the excess polycations, and $S_{pos}(q)$ grows at small q as a result. The trend is reversed for system 10, possessing equivalent amounts of polycations and polyanions. This can be rationalized by the fact that translational entropy (rule IV) favors a division of larger clusters into several smaller ones. There is no longer any excess charge to share, and the electrostatic correlation attraction between small *neutral* clusters is apparently not sufficiently strong to firmly bring them together. Note that even if no salt is added, the counterions give rise to a concentration of small-ion pairs of about 0.08 M and a screening length of 10.5 Å, which is short even on the scale of a polyion.

So far, all chains have had the same length and absolute charge, while some polydispersity would be expected in a real system. To examine this further and to make a closer connection with experimental systems, we also considered model systems containing (i) polyions with a length polydispersity and (ii) polycations and polyanions of slightly unequal length. On the basis of system 10, three systems with increasing polydispersity have been constructed. The same chain length distribution, which is symmetric around 20 monomers, has been applied to the polycations and polyanions, and these three systems are referred to as 181, 262, and 12421, respectively (see Table 2 for details). The other extension to system 10 is a system containing 9 polycations with 22 charged beads and 11 polyanions with 18 charged beads, referred to as system 9(22):11(18). In all four additional systems, each bead carries one elementary charge and all these systems possess equal numbers of positively and negatively charged beads as in system 10.

Figure 4 shows that $S_{pos}(q)$ increases at $q = q_{low}$ as the polydispersity is increased among systems 181, 262, and 12421. Hence, a formation of larger clusters is promoted as the polydispersity is increased. Moreover, system 9(22):11(18) displays an even larger value of $S_{pos}(q)$ at small q. According to rule II, a preference for clusters of low charge density is expected, and the lowest possible charge density appears obviously for neutral complexes. In a polydisperse system, there are fewer combinations of pairs of polyions with matching charge, and consequently, the probability of small neutral clusters is decreased and the probability of larger clusters is increased. This is brought to the extreme in system 9(22):11(18), where the only possibility of creating a neutral cluster is by forming a complex involving *all* polyions.

However, polydispersity could also introduce an opposing effect. Polydispersity allows the formation of clusters with an absolute charge much smaller than the absolute charge of a single polyion. That would make it easier to break rule I, since the energetic penalty of having clusters of opposite charge would be reduced compared to monodisperse systems. Thus, there could be a larger variety of small clusters with small absolute charge of opposite sign, which would be favored by rule IV. As seen in Figure 4, the net effect of polydispersity is an enhanced clustering, which again leads to the conclusion that the energetic consideration, rule I in this case, is more important.

5.2. Added Salt. The ionic strength of the solution is an important property in experimental systems. In our screened Coulomb approach, addition of salt is taken into account via the screening length κ^{-1}. As salt is added, κ^{-1} is decreased and the electrostatic attraction between oppositely charged beads is reduced (see eq 2). Hence, the driving force for forming clusters will decrease and the promotion of smaller cluster by the translational entropy will become important.

An alternative description would be to use explicit ions and a Coulomb potential. This would change the short-range interactions and add correlations. In our previous paper,[26] we compared the two models and found a very good agreement. Apparently, the different effects cancel each other to some degree. For the addition of salt, we would expect explicit ions to give slight shifts in properties such as cluster distributions and structure factors, compared to the screened Coulomb results, but the general trends should be the same.

The effect of salt on the clusters will be investigated using system 5 (which in the absence of added salt is dominated by 2:1 clusters), system 9 (large charged clusters), and system 10 (neutral clusters). In the following, the discussion will start from the very high salt regime (low κ^{-1}) and end with no salt added (κ^{-1} = 12.1, 10.7, and 10.5 Å, respectively).

5.2.1. System 5. The probability of the most important clusters in system 5 as a function of κ^{-1} is given in Figure 5. In the case of complete screening, $\kappa^{-1} = 0$, the 1:0 and 0:1 clusters dominate ($P_{1,0} = 0.50$ and $P_{0,1} = 0.25$), whereas at $\kappa^{-1} = 4$ Å, the 1:1, 1:0, and 2:1 clusters are the most probable ones. As κ^{-1} is further increased, $P_{2,1}$ increases monotonically at the expense of $P_{1,1}$ and $P_{1,0}$. Significant amounts of 3:2 and 4:2 clusters also appear with maximal probabilities at $\kappa^{-1} \approx$ 6−8 Å.

As long as the electrostatic interactions are weak, the polyions stay mostly free. The remaining fraction of multipolyion clusters

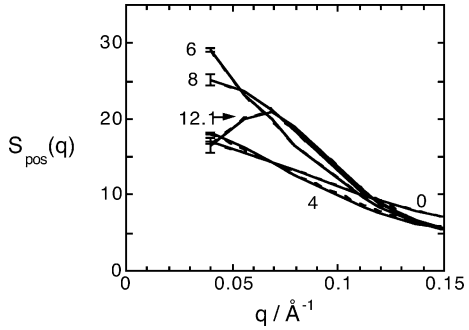

Figure 6. Structure factors of the positive beads $S_{pos}(q)$ calculated from eq 6 (solid lines) and eqs 7−9 (dashed lines) for system 5 at indicated κ^{-1} (in Å). The solid and dashed curves overlap almost completely. Statistical uncertainties, which decrease as q is increased, are given at $q = q_{min}$.

is due to a nonzero density. As κ^{-1} is increased, the electrostatic interactions become more important and the first complex formed is the 1:1 cluster, whereas at $\kappa^{-1} = 4$ Å also the 2:1 cluster starts to appear. Hence, at this stage the energetic preference of sharing the excess charge of one polycation among three polyions in a 2:1 cluster (rule II) becomes more important than the entropic gain (rule IV) of having a charged 1:0 cluster and a neutral 1:1 cluster.

Figure 6 displays the partial structure factor $S_{pos}(q)$ at different values of κ^{-1}. The partial structure factor has been evaluated using eq 6 and using eqs 7−9, separately. We will first examine the structure factors and thereafter compare the two approaches.

As seen in Figure 6, at small q, $S_{pos}(q)$ initially increases, reaches a maximum at $\kappa^{-1} \approx 6$ Å, and then becomes attenuated at $q < 0.07$ Å^{-1} for larger κ^{-1}. The general increase of $S_{pos}(q)$ as κ^{-1} is increased is again a manifestation of the association of polycations into complexes held together with polyanions. At nonzero, small κ^{-1}, the electrostatic interactions are short-ranged and local on the scale of a cluster but strong enough to establish clusters with more than one polycation, primarily 2:1 but also 3:2 and 4:2 clusters. Cluster−cluster interactions can be described as being "sticky" due to short-range correlation attractions, which give rise to the association and a large $S_{pos}(q)$ at small q. The complexes that form at the expense of 1:0 and 1:1 clusters have a net charge, which becomes important when the interactions become long-ranged. Thus, as κ^{-1} increases further, the mutual electrostatic repulsion causes a strong separation between the charged complexes, which now dominate the solution, and a peak is formed in the partial structure factor. This will be discussed further below.

The partial bead structure factors evaluated through eq 6 (solid lines) and through eqs 7−9 (dashed lines) are both included in Figure 6. There is an almost complete agreement, demonstrating that the factorization of the bead structure factor into a polycation form factor and a polycation structure factor is an excellent approximation in the present systems. Hence, the scattering properties can accurately be described as a combination of a particle form factor and a particle structure factor.

The polycation form factor $F_{pos}(q)$ is shown for various κ^{-1} in Figure 7. A reduction of $F_{pos}(q)$ appears as κ^{-1} is increased from 0 to 4 Å, implying a weak spatial expansion of the polycation. Note that the hard-sphere diameter is also 4 Å, but the electrostatic interactions are slightly more long-ranged, since they are not completely screened at this distance, even though $\kappa^{-1} = 4$ Å. From this point, $F_{pos}(q)$ becomes independent of κ^{-1}, indicating that the polycation conformation is insensitive to the change of the polyion environment as the polyion shifts from being free or in 1:1 clusters to form 2:1 clusters. In a

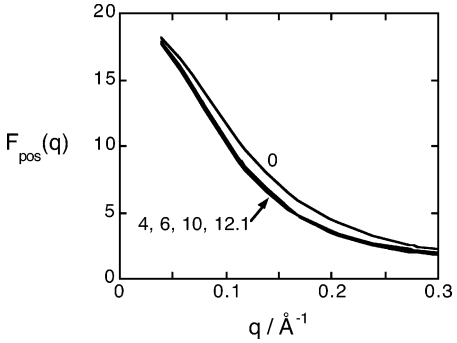

Figure 7. Polycation form factors $F_{pos}(q)$ for system 5 at indicated κ^{-1} (in Å).

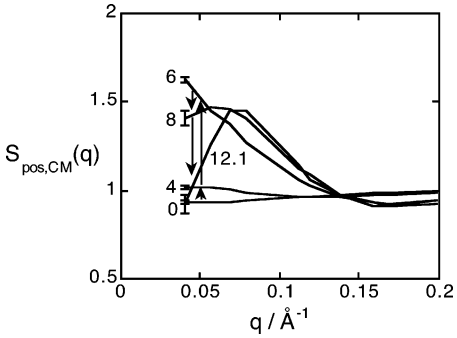

Figure 8. Polycation structure factors $S_{pos,CM}(q)$ for system 5 at indicated κ^{-1} (in Å). The functions are based on the positions of the centers of mass of the polycations. Statistical uncertainties, which decrease as q is increased, are given at $q = q_{min}$. The arrows show the order of increasing κ^{-1}.

cluster, we have both (i) *attraction* between the beads of opposite charge (making the polycations more contracted/less extended) and (ii) *repulsion* between beads of same charge (making the polycations less contracted/more extended). It is conceivable that these two effects are able to cancel each other and that the correlations within a 2:1 cluster create an environment corresponding to a short effective screening length.

Figure 8 shows the polycation structure factor $S_{pos,CM}(q)$ as a function of q for various κ^{-1}. Since (i) eq 7 was an excellent approximation and (ii) $F_{pos}(q)$ was insensitive to κ^{-1}, the variation of $S_{pos,CM}(q)$ across different κ^{-1} resemble that of $S_{pos}(q)$, but the interpolycation structure is more prominent when the form factor is removed. At $\kappa^{-1} = 0$, $S_{pos,CM}(q) < 1$ at small q values, indicating a weak net repulsion among the chains due to the hard-sphere bead−bead repulsion. The effective chain−chain repulsion is soft, however, as a consequence of the flexibility of the chains. At $\kappa^{-1} = 4$ Å, $S_{pos,CM}(q) \approx 1$ at all q values, and hence, the hard-sphere repulsion is matched by an effective electrostatic attraction between polycations mediated by polyanions. As κ^{-1} is further increased, the polycation structure factor grows at small q, which reflects the increasing number of polycations located in complexes with more than one polycation. At $\kappa^{-1} = 8$ Å, the polycation structure factor has saturated for $q > 0.06$ Å^{-1}, where it starts to primarily represent the internal structure (center-of-mass correlations) of the dominating 2:1 clusters (cf. Figure 5). As the electrostatic interactions become stronger and more long-ranged, $S_{pos,CM}(q)$ decreases for $q < 0.06$ Å^{-1} due to the cluster−cluster repulsion and a prominent peak is formed. In other words, for a longer screening length, the system is characterized by an association of pairs of polycations into complexes (with a polyanion) with the complexes repelling each other.

The polycation−polycation radial distribution functions, $g_{pos,CM}(r)$, offer another viewpoint to same events and are

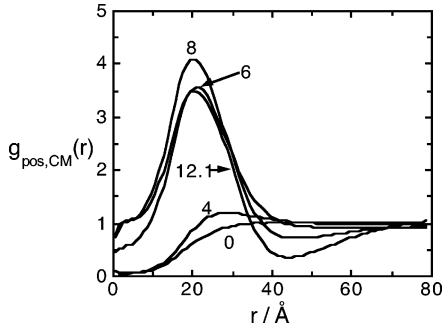

Figure 9. Polycation−polycation radial distribution functions $g_{pos,CM}(r)$ for system 5 at indicated κ^{-1} (in Å). The functions are based on the positions of the centers of mass of the polycations.

displayed in Figure 9. The uncharged system shows a correlation hole at short separations ($r < 25$ Å) due to the excluded volume of the polycations, which is comparable to twice the radius of gyration (2×13.4 Å $= 26.8$ Å). At large separations, spatial correlations vanish and $g_{pos,CM}(r)$ approaches 1. A peak occurs at $r \approx 25$ Å and grows drastically in the interval $\kappa^{-1} = 4-6$ Å, indicating that the density of polycations in close proximity increases. From the cluster analysis, this range corresponds to a switching of dominating clusters from 1:0 and 1:1 to 2:1 together with 3:2 and 4:2 clusters (Figure 5). At $\kappa^{-1} = 8$ Å, the height of the peak reaches its largest value and a broad minimum appears at 40−50 Å, which shows that the density of polycations decreases in a nearby region, reflecting that complexes start to repel each other. At $\kappa^{-1} = 12.1$ Å (salt-free case), the maximum of $g_{pos,CM}(r)$ is reduced and the minimum becomes more pronounced. These effects are associated with the decline of larger complexes, such as 3:2 and 4:2 clusters, in favor of 2:1 and the growing strength and range of the repulsion between complexes, respectively.

Let us take a closer look at the phasing out of complexes larger than 2:1 clusters. The loss of 3:2 clusters when electrostatic interactions are becoming increasingly important is consistent with rule II, as quantified by eq 12. Since the polycation−polyanion ratio of the whole system is 2:1, a 3:2 cluster can be seen as requiring a free polycation, i.e., a 1:0 cluster to make up the system ratio. According to eq 12, the summed energy of a 3:2 and a 1:0 cluster is 1.8 times higher than that of two 2:1 clusters.

The fact that the probability of 4:2 clusters decreases when electrostatic interactions are increased demonstrates that there is also an energetic driving force, besides the entropic one (rule IV), that promotes clusters of a small net charge. This is expressed in rule III, which accounts for extra repulsion between excess polyions in a cluster, beyond the approximations contained in eq 12. Although eq 13 is expected to exaggerate the effect, it gives a hint about the mechanism.

Combined, the rules would predict that the system wants to break up into clusters having one excess polyion and the same composition as the system as a whole, i.e., the same polycation−polyanion ratio. This is possible in system 5, which explains the overwhelming dominance of 2:1 clusters in the salt-free case.

5.2.2. System 9. The effect of salt on system 9 will now be considered. Figure 10a and b show the cluster size probability distributions at $\kappa^{-1} = 4$ and 6 Å, respectively. The distribution at $\kappa^{-1} = 10.7$ Å was shown in Figure 2b. At $\kappa^{-1} = 0$, the cluster size probability distribution is very similar to that of system 5, mainly displaying free polyions. At $\kappa^{-1} = 4$ Å with only weak electrostatic interactions, neutral 1:1 and 2:2 clusters dominate (Figure 10a). The positively charged clusters 1:0 and 2:1 are also present to a significant degree and so are their oppositely

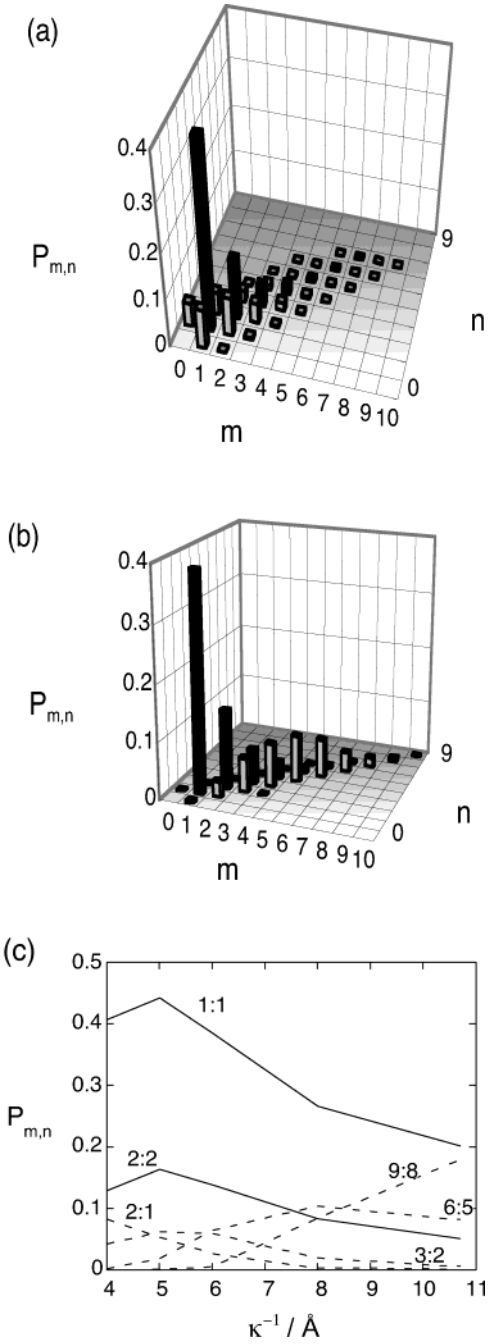

Figure 10. (a and b) Cluster size probability distribution $P_{m,n}$ vs the number of polycations m and the number of polyanions n in polyion complexes for system 9 at (a) $\kappa^{-1} = 4$ Å and (b) 6 Å. Neutral clusters are represented by black columns and charged clusters by gray columns. (c) Cluster size probability distribution $P_{m,n}$ vs screening length κ^{-1} for system 9 and selected cluster compositions as indicated. Solid lines are used for neutral clusters and dashed lines for charged clusters.

charged counterparts 0:1 and 1:2. Moreover, there are minor contributions from a large variety of other clusters. At $\kappa^{-1} = 6$ Å, the negative clusters have almost disappeared as would be expected (rule I). There is still a large probability for small neutral complexes, whereas the probability for positively charged clusters has shifted to larger ones with a broad distribution centered between 4:3 and 5:4 clusters (Figure 10b). Finally, at $\kappa^{-1} = 10.7$ Å, the shift to larger positively charged clusters has been continued (Figure 2b). Due to the constraints of the system, this is accompanied by a reduction of the probabilities for the small neutral clusters. Without negatively charged clusters, there can be only one charged cluster, since there is an excess of

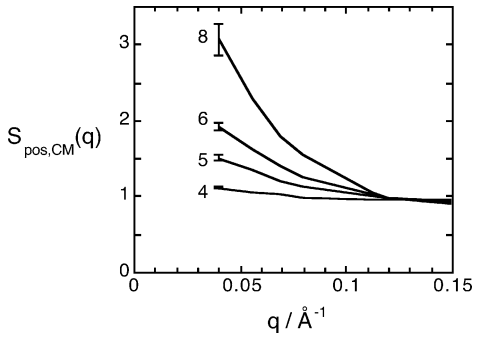

Figure 11. Polycation structure factors $S_{pos,CM}(q)$ for system 9 at indicated κ^{-1} (in Å). The functions are based on the positions of the centers of mass of the polycations. Statistical uncertainties, which decrease as q is increased, are given at $q = q_{min}$.

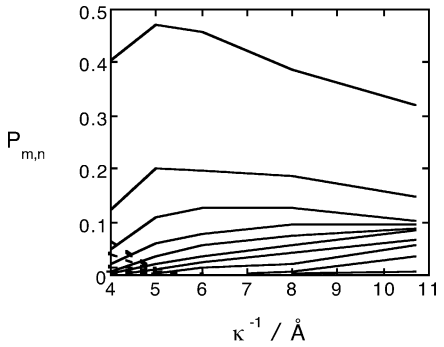

Figure 12. Cluster size probability distribution $P_{m,n}$ vs screening length κ^{-1} for system 10 and selected cluster compositions including neutral clusters from 1:1 to 10:10 (solid lines, top to bottom) and the charged clusters 1:0, 2:1, 3:2, and 4:3 (dashed lines, top to bottom).

only one polycation. The other complexes are neutral, and as the charged complex grows with increasing κ^{-1}, collecting more polycation−polyanion pairs, the probabilities of the neutral clusters must decrease.

The general trends as κ^{-1} is increased, i.e., the gradual transition from small (2:1) to large (9:8) positively charged clusters together with the loss of neutral 1:1 and 2:2 clusters, are also illustrated in Figure 10c, which shows the probabilities of selected clusters. (For clarity not all charged clusters are included in the plot.)

The polycation structure factor $S_{pos,CM}(q)$ at different κ^{-1} is shown in Figure 11. At low κ^{-1}, there is very little structure and again the chains are nearly homogeneously distributed. As κ^{-1} is increased, the magnitude at small q increases continuously due to the net attraction and aggregation represented by the growth of the charged cluster.

Thus, when the electrostatic interactions are turned on, the first step is an association between oppositely charged polyions and small neutral clusters are formed. When κ^{-1} is further increased, it becomes more favorable for the polyions to share the excess charge of the extra polycation and distribute it in larger clusters. As before, when the electrostatic interactions are increased in strength and range, the relative importance of energetic considerations (rule II) is increased relative to entropic ones (rule IV).

5.2.3. System 10. Figure 12 shows the cluster size probability distribution as a function of κ^{-1} for system 10 for selected cluster compositions. At $\kappa^{-1} = 4$ Å, the cluster size distribution is similar to that for system 9 with a dominance of 1:1 and 2:2 clusters, which coexist with small charged ones. The full cluster size probability distribution resembles that of Figure 10a, and since there is an equal number of polycations and polyanions, there is also perfect symmetry with respect to the existence of clusters of opposite charge. As κ^{-1} is increased, there is first an increase of the probability of small neutral clusters. $P_{1,1}$ and $P_{2,2}$ have maxima at $\kappa^{-1} \approx 5-6$ Å and $P_{3,3}$ at $\kappa^{-1} \approx 7$ Å. At the same time, charged clusters vanish (dashed lines). Hence, at larger κ^{-1} only neutral clusters exist. The probability of the small ones decreases and that of larger ones increases. The full distribution at $\kappa^{-1} = 10.5$ Å was given in Figure 2c. From Figure 12 we also infer that as counterions would be removed from the system ($\kappa^{-1} > 10.7$ Å), small neutral clusters would gradually merge into larger ones. The trends observed for system 10 are in agreement with rules I−IV.

Finally, the polycation structure factor $S_{pos,CM}(q)$ for system 10 increases monotonically as the electrostatic interactions are increased (not shown), similar to that shown in Figure 11 for system 9. However, the maximum value of $S_{pos,CM}(q)$ at $q = q_{low}$ is smaller, e.g., 1.9 compared to 3.1 at $\kappa^{-1} = 8$ Å, since system 10 has many small clusters in contrast to the tendency in system 9 to collect a large part of the system into at least one big aggregate.

6. Conclusions

On the basis of a simple spring-bead model representing a solution of oppositely charged polyions studied by Monte Carlo simulations, the formation of polyion complexes and the structure of the solution have been examined. With a fixed amount of polycations at constant volume, the number of polyanions and the amount of added salt have been varied.

It was found that the propensity for cluster formation could be rationalized by four simple rules. For electrostatic reasons, (I) a coexistence of oppositely charged clusters is unlikely and (II) charged clusters prefer to be large with (III) a low absolute net charge, whereas from an entropic point of view (IV) many and consequently smaller clusters are preferred.

In the absence of added salt, when the screening comes only from the counterions of the polyions, the electrostatic energy dominates over entropy. In system 5, which contains 10 polycations and 5 polyanions with the same absolute charge, the scene is dominated by 2:1 clusters, kept apart by a net repulsion. Close to an equivalent amount of polyions, there is an increasing propensity to form large clusters. This may be seen as the excess polycations collecting the available neutral pairs of positive and negative polyions to share the excess charge, although small neutral clusters still appear for entropic reasons. The largest complex is, thus, observed when there is only one excess polycation.

When equal amounts of polyions are present, neutral clusters of small to intermediate size dominate the system, since, at the present conditions, the attractive electrostatic correlation interactions between neutral clusters do not yet dominate over the entropy. The trend, however, is that the proportion of large neutral clusters would be higher for longer screening lengths than investigated here. Small neutral clusters are favored by the fact that all chains are of equal length and absolute charge. If the polyions are made polydisperse or if polycations and polyanions have unequal length (and hence unequal absolute charges), the propensity for forming larger clusters is increased considerably in a system with equal amounts of positive and negative polyion charges. Here, the likelihood of small neutral clusters is reduced or even completely eliminated for combinatorial reasons. In the latter case, with polycations and polyanions of unequal length and charge, large clusters cannot be split up into small ones without creating oppositely charged clusters at a substantial cost in electrostatic energy.

The addition of salt was investigated by varying the screening length. When the screening length is short, the electrostatic interactions are reduced and rules I−III become less significant in relation to rule IV. This is, e.g., manifested by a larger fraction of smaller clusters. Also, clusters of opposite charge may be present. Moreover, the attractive interactions, which lead to associations into complexes, and the repulsion between charged complexes are characterized by different length scales and are, thus, affected differently by the variation of the screening length. In system 5 an intermediate regime is found where 2:1 clusters dominate but repel each other only weakly or even show some net (correlation) attraction, due to the short-range nature of the interactions.

Finally, the factorization of the bead structure factor, which represents the correlations between individual polycation beads, into a polycation form factor and a center-of-mass structure factor was found to be an excellent approximation, implying that intra- and interchain correlations are practically uncoupled. In fact, the polycation form factor was independent of variations in the screening length as long as the latter was equal to the hard-sphere diameter or longer, while the cluster size distribution and the center-of-mass structure factor underwent substantial changes.

Acknowledgment. Y.H. thanks T. Kawakatsu and U. Olsson for a series of stimulating discussions. The work was supported by grants from the Foundation of Strategic Research (SSF) and the Swedish National Research Council (NFR).

References and Notes

(1) Bakeev, K. N.; Izumrudov, V. A.; Kuchanov, S. I.; Zezin, A. B.; Kabanov, V. A. *Macromolecules* **1992**, *25*, 4249.
(2) Kabanov, V. A. *Polym. Sci.* **1993**, *36*, 143.
(3) Kabanov, A. V.; Bronich, T. K.; Kabanov, V. A.; Yu, K.; Eisenberg, A. *Macromolecules* **1996**, *29*, 6797.
(4) Kabanov, V. A.; Zezin, A. B.; Rogacheva, V. B.; Gulyaeva, Z. G.; Zansochova, M. F.; Joosten, J. G. H.; Brackman, J. *Macromolecules* **1999**, *32*, 1904.
(5) Kabanov, V. A. Fundamentals of Polyelectrolyte Complexes in Solution and the Bulk. In *Multilayer Thin Films; Sequential Assembly of Nanocomposite Materials*; Decher, G., Schlenoff, J. B., Eds.; Wiley: New York, 2003.
(6) Pogodina, N. V.; Tsvetkov, N. V. *Macromolecules* **1997**, *30*, 4897.
(7) Takahashi, S.; Yoshikawa, K.; Vasilevskaya, V. V.; Khokhlov, A. R. *J. Phys. Chem. B* **1997**, *101*, 9396.
(8) Yamasaki, Y.; Teramoto, Y.; Yoshikawa, K. *Biophys. J.* **2001**, *80*, 2823.
(9) Makita, N.; Yoshikawa, K. *Biophys. Chem.* **2002**, *99*, 43.
(10) Minagawa, K.; Matsuzawa, Y.; Yoshikawa, K.; Matsumoto, M.; Doi, M. *FEBS Lett.* **1991**, *295*, 67.
(11) Kidoaki, S.; Yoshikawa, K. *Biophys. J.* **1996**, *71*.
(12) Ladam, G.; Schaad, P.; Voegel, J. C.; Schaaf, P.; Decher, G.; Cuisinier, F. *Langmuir* **2000**, *16*, 1249.
(13) Michel, E.; Gero, D. *Nano Lett.* **2001**, *1*, 45.
(14) *Fundamentals of Polyelectrolyte Complexes in Solution and the Bulk*; Decher, G., Schlenoff, J. B., Eds.; Wiley: New York, 2003.
(15) Dautzenberg, H. *Macromolecules* **1997**, *30*, 7810.
(16) Christos, G. A.; Carnie, S. L. *J. Chem. Phys.* **1990**, *92*, 7661.
(17) Stevens, M. J.; Kremer, K. *Macromolecules* **1993**, *26*, 4717.
(18) Stevens, M. J.; Kremer, K. *Phys. Rev. Lett.* **1993**, *71*, 2228.
(19) Stevens, M. J.; Kremer, K. *J. Chem. Phys.* **1995**, *103*, 1669.
(20) Stevens, M. J.; Kremer, K. *J. Phys. II France* **1996**, *6*, 1607.
(21) Valleau, J. P. *J. Chem. Phys.* **1989**, *129*, 163.
(22) Christos, G. A.; Carnie, S. L. *Chem. Phys. Lett.* **1990**, *172*, 249.
(23) Woodward, C. E.; Jönsson, B. *J. Chem. Phys.* **1991**, *155*, 207.
(24) Ullner, M.; Woodward, C. E. *Macromolecules* **2000**, *33*, 7144.
(25) Winkler, R. G.; Steinhauser, M. O.; Reineker, P. *Phys. Rev. E* **2002**, *66*, 021802.
(26) Hayashi, Y.; Ullner, M.; Linse, P. *J. Chem. Phys.* **2002**, *116*, 6836.
(27) Metropolis, N.; Rosenbluth, A. W.; Rosenbluth, M. N.; Teller, A. H.; Teller, E. *J. Chem. Phys.* **1953**, *21*, 1087.
(28) Allen, M. P.; Tildesley, D. J. *Computer Simulation of Liquids*; Oxford: New York, 1987.
(29) Linse, P. MOLSIM, 3.0 ed.; Lund University: Sweden, 2000.